HAYATI
Journal of Biosciences

Vol. 32 No. 1, January 2025 47-54
DOI:10.4308/hjb.32.1.47-54
ISSN: 1978-3019
EISSN: 2086-4094

Research Article

Characterisation of ACE2-like Enzyme from *Bacillus cereus* sp. as an Alternative Treatment for COVID-19 Patients

Alya Sendra Maulida, Novi Arie Anggraeni, Azzania Fibriani*

School of Life Sciences and Technology, Institut Teknologi Bandung (ITB), Bandung 40132, Indonesia

ARTICLE INFO

Article history:
Received July 30, 2024
Received in revised form September 12, 2024
Accepted October 8, 2024

KEYWORDS:
ACE2-like enzyme,
COVID-19,
SARS-CoV-2,
Bacillus cereus sp.,
M32-Carboxypeptidase

ABSTRACT

SARS-CoV-2 infection can lead to downregulation of ACE2, raising pro-inflammatory Angiotensin II levels. Recombinant human ACE2 protein therapy can restore homeostasis but is costly. An alternative is an ACE2-like enzyme with similar effects. The previous research identified a carboxypeptidase protein from *Bacillus cereus* sp. (rBceCP) as a potential ACE2-like enzyme, but it has not been characterized well. This study characterizes, expresses, and tests the activity of the rBceCP). rBceCP structure and properties were predicted using Prabi and Expasy. The *in vitro* approach included protein expression optimization, hydrolysis tests, and inhibition tests. *In silico* analysis revealed the protein is a homodimer with 53.66% α-helix and a molecular weight of 58.99 kDa. The protein is stable, hydrophilic, and has an isoelectric point at pH 4.93, indicating it can be expressed using the *E. coli* system. Expression of rBceCP showed no significant differences across IPTG concentrations (p-value >0.05). The protein hydrolysis activity of rBceCP was similar to the control, though purified samples had lower activity than crude samples. Inhibition activity in crude and purified samples showed no significant differences (p-value >0.05) and was higher than the control. Thus, rBceCP has potential as an ACE2-like enzyme and a therapeutic candidate for COVID-19.

1. Introduction

Angiotensin-converting enzyme 2 (ACE2) shares a similar amino acid sequence with Angiotensin-converting enzyme (ACE). However, ACE can act as a negative regulator for ACE2. Both enzymes are essential in the renin-angiotensin system (RAS), which maintains blood pressure and fluid balance. When RAS is activated, the angiotensin-converting enzyme (ACE) alters the deca-peptide angiotensin I, also known as Ang I or Ang (1–10), by removing its C-terminus, leading to the creation of the vasopressor octa-peptide, angiotensin II (also labeled as Ang II or Ang 1–8). Within the RAS, ACE2 functions to regulate Ang II concentrations by transforming it into angiotensin 1–7 (Ang 1–7), thereby counterbalancing the effects of ACE (Donoghue *et al.* 2000; Tipnis *et al.* 2000). As the production of Ang II can exacerbate the symptoms of Acute Respiratory Distress Syndrome (ARDS), a frequent complication seen in about 67% of COVID-19 patients, it is significant to note its role in the disease's progression (Imai *et al.* 2005; Yang *et al.* 2020; Meyer *et al.* 2021).

The tissue targeting and host range of SARS-CoV-2 is primarily determined by its spike protein. SARS-CoV-2 competes with Ang II for ACE2 during the process of internalization. However, this competition inhibits ACE2 functionality to hydrolyze the Ang II and amplifies the harmful activation of the ACE/Ang II pathway. This results in heightened vasoconstriction due to Ang II and reduced vasodilation influenced by Ang (1–7) (Muslim *et al.* 2020; Yamaguchi *et al.* 2021). Therefore, many researchers have developed recombinant soluble human ACE2 (rshACE2) as a therapy for ARDS patients. However, using rshACE2 requires a very high cost because it uses a protein expression system within mammalian cells (Khan *et*

* Corresponding Author
E-mail Address: afibriani@itb.ac.id

al. 2017). Thus, other alternatives must be developed to replace rshACE2 without reducing its therapeutic effect.

Based on the research study by Minato *et al.* (2022), a carboxypeptidase (CAP) enzyme that belongs to the M32-Carboxypeptidase family derived from *Paenibacillus* sp. B38 (B38 CAP) has been found to have similar activity as the ACE2 enzyme (Minato *et al.* 2022). In addition, this protein expression system can also be carried out using bacterial cells so that it can be mass-produced as an ACE2-like enzyme and is more practical than rshACE2. Therefore, the utilization of ACE2-like enzyme as a therapy for COVID-19 patients has the potential to be further developed.

From a previous study by Izza (Laily *et al.* 2023) it was found that *Enterobacter* sp. 200527-13 as a LAB bacteria has an enzyme with ACE2-like activity in the form of carboxypeptidase (EntCP) that belongs to the M32-Carboxypeptidase family. By using the fluorescent substrate Nma-His-Pro-Lys(Dnp), which can mimic angiotensin, it is known that EntCP has hydrolysis activity similar to ACE2. In a follow-up study conducted by Fibriani (Fibriani *et al.* 2022), it was also discovered that the *Bacillus cereus* bacteria had the same activity (rBceCP). This study aims to characterize recombinant BceCP (rBceCP) and evaluate its inhibitory activity against the SARS-CoV-2 Spike protein.

2. Materials and Methods

2.1. Structure and Psychochemical Character Analysis of Protein rBceCP

The protein structure was modeled with Homology Modeling (SWISS-MODEL (expasy.org)). The secondary structure of the protein was analyzed at npsa-prabi.ibcp.fr. The psychochemical character of the protein was analyzed on the Expasy website with ProtParam (http://web.expasy.org/protparam/) (Satyanarayana *et al.* 2018) and the hydropathy of protein was analyzed using the Kyte-Doolittle Hydropathy Plot version 2.0u66.

2.2. Recombinant BceCP Expression

The BceCp-coding g ene (1,516 bp) was synthesized and cloned into the pET21b(+) backbone plasmid (6,891 bp) by Integrated DNA Technologies (IDT) (Figure 1). The integrity of the rBceCP coding sequence was confirmed through DNA sequencing. Transformant colonies were picked and inoculated onto Luria Bertani medium containing ampicillin. The culture was incubated until OD_{600} reached ~0.5-0.8 (mid-log phase). IPTG was added at 0, 0.25, 0.5, and 1 mM to induce protein expression. The culture was incubated for 3 hours at 37°C with shaking at 150 rpm. The sample was then centrifuged at 6,000xg for 10 minutes at 4°C. The resulting pellet was weighed, and each 0.02 g pellet was resuspended with 100 µL of buffer containing 2M imidazole for further cell lysis by sonication using an Omni Ruptor 4,000 ultrasonic homogenizer. The resulting supernatant and pellet fractions were aliquoted and visualized by SDS-PAGE (separating gel 12% and stacking gel 4%). A comparison of the density of protein bands resulting from induction by various concentrations of IPTG was then measured with the ImageJ program to estimate the proportion of protein concentration produced.

2.3. Protein Purification

Three milliliters of rBceCP protein were placed into the Ni-NTA column (HisPur™, Thermo Fisher) and incubated for 90 minutes on an orbital shaker to facilitate binding. The column was washed seven times with 2 ml of wash buffer. Finally, the protein was eluted from the column six times by adding 2 ml of elution buffer. The histidine-tagged rBceCP was then eluted using an imidazole gradient. Fractions with purified rBceCP were concentrated to 1-2 mg/ml using Ultra 15 ml centrifugal filters ten kDa (Amicon®, Merck). Protein aliquots were preserved at -20°C.

2.4. Wester Bloting Analysis

The SDS-PAGE gel with purified rBceCP in it was rinsed with equilibration buffer for one minute, while the PVDF membrane was soaked in methanol for 15 minutes and then rinsed again with equilibration buffer for a further minute. The stack of sponge, gel, and membrane was flattened using a roller to eliminate any air bubbles that may have formed. Blotting was conducted for five minutes in three cycles. Subsequently, the membrane was immersed in a 1% blocking solution at room temperature with agitation for one hour, after which it was incubated with mouse anti-His tag IgG at 4°C for 16 hours. Subsequently, the membrane was rinsed with TBS-T on three occasions and incubated with HRP-conjugated goat anti-mouse IgG at room temperature with agitation for one hour. A further three rinses with TBS-T followed this. The results were analyzed using chemiluminescence. Subsequently, the blotted membrane was incubated with WesternSure®

PREMIUM Chemiluminescent Substrate, which was prepared by mixing a stable peroxide solution and a luminol enhancer solution in a 1:1 ratio. A recombinant protein derived from *Enterobacter* sp. was used as positive control.

2.5. rBceCP Protein Hydrolysis and Inhibition Activity Assay

The crude and purified proteins (150 µL or 250 µg/ml) obtained from the harvest were subjected to hydrolysis activity testing using the Nma-His-Pro-Lys (Dnp) substrate, following the techniques provided by Peptide Institute (Laily *et al.* 2023). The inhibition assay was employed to analyze the SARS-CoV-2 S1 Protein-ACE2 Binding Inhibitor Screening Kit (Abcam) to conduct an inhibition experiment. The inhibition activity was then calculated according to the protocol on the kit.

$$\text{Relative inhibition} = \frac{(\text{OD[Binding]} - \text{OD[Sample]})}{\text{OD[Binding]}} \times 100$$

2.6. Data Analysis

The data obtained were statistically tested using IBM SPSS Statistics (ver. 24). Significance test was performed with t-test and Kruskal-Wallis. Variations in average values were deemed significant when $p<0.05$.

3. Results

3.1. Characteristics of rBceCP

The rBceCP visualization is shown in Figure 2A with a template in the form of a crystal structure of the M32-CAP protein from *Bacillus subtilis* (3HQ2). Based on the modeling, rBceCP formed a homodimer with the most dominating secondary structure, α-helix. Its proportion reaches 53.66% of the protein's overall structure, followed by a random coil of 38.22% and an extended strand of 8.12%. The Ramachandran Plot evaluated the protein model and demonstrated that 97.78% of the total amino acids were in the

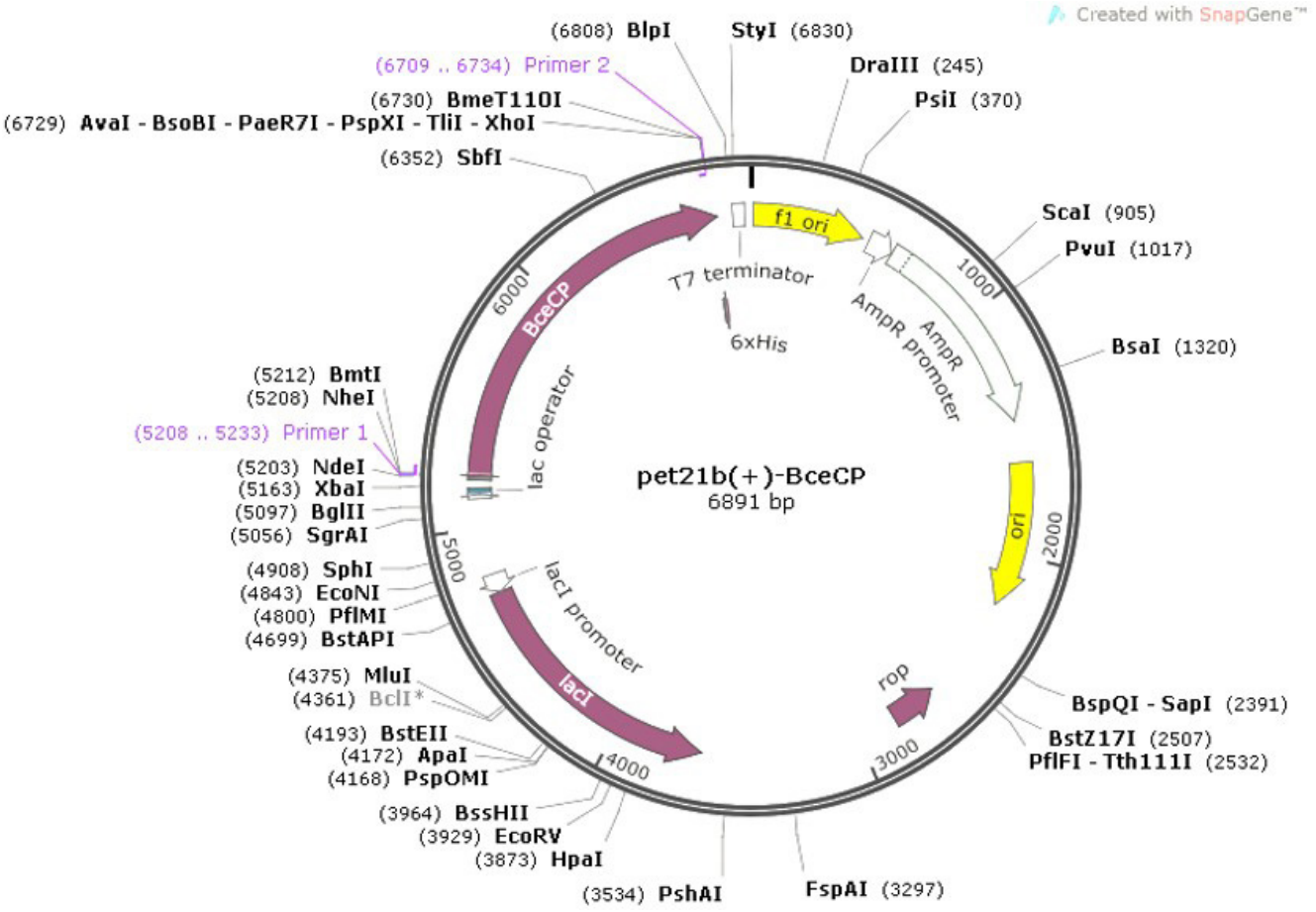

Figure 1. pET21b(+)-BceCP plasmid construct

favorable/allowed region, and the remaining 0.3% were outliers (Figure 2). These results indicate that the modeled protein structure has good conformation and stereochemical quality.

The results of the hydrophobicity analysis can be seen in Figure 2C. Based on the plot, it can be seen that most of the amino acid residues that make up the rBceCP are hydrophilic. This can be seen from the peaks on the graph, which are more in the negative scale area (towards H_2O) than the positive scale area (towards CH_3). The hydropathy scale value on the Kyte-Doolittle plot obtained for each amino acid residue that makes up the rBceCP is then calculated by summing the scale value and dividing it by the total amino acid residues that make up the protein so that the GRAVY value is obtained in Table 1.

Based on the psychochemical character analysis, 505 amino acids comprised the rBceCP with the protein formula C2667H4070N670O806S18. However, the predicted molecular weight of rBceCP increased to 60.3 kDa by adding a 6xHis tag on the plasmid from 58.99 kDa. The GRAVY value of the rBceCP obtained is negative, with a value of -0.571, so the protein was classified as hydrophilic. The Aliphatic Index (AI) that

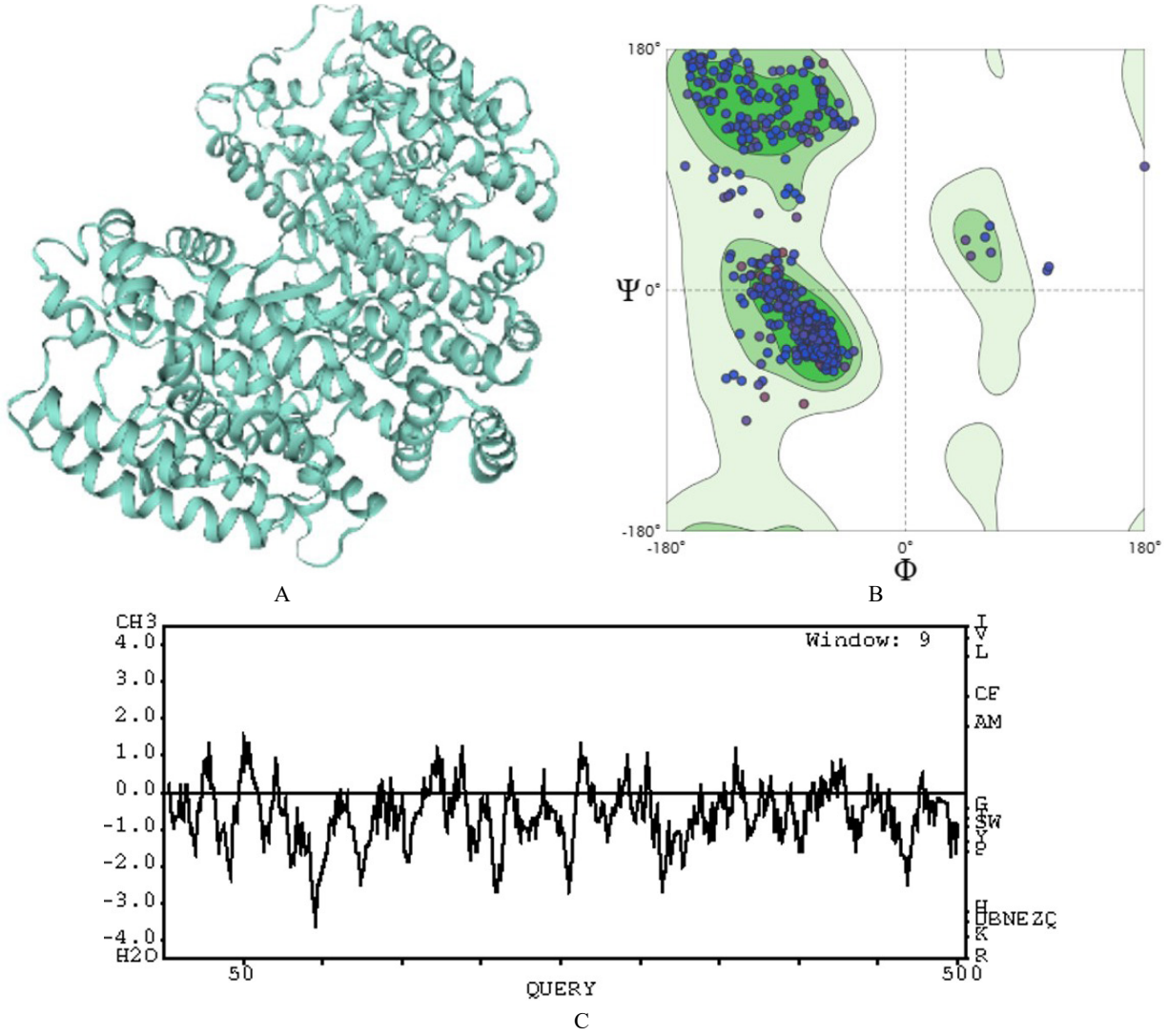

Figure 2. (A) Structure modeling visualization of rBceCP, (B) ramachandran plot of 3D model of rBceCP, (C) hydropathy plot of rBceCP

Table 1. Psychochemical characterization of CAP protein from *Bacillus cereus*. [a]Amino acid count, [b]Molecular weight, [c]Isoelectric point, [d]Instability index, [e]Grand average of hydropathy, [f]Negatively charged amino acid residues, [g]Positively charged amino acid residues, [h]Aliphatic index

Nama	AA[a]	MW[b]	pI[c]	II[d]	GRAVY[e]	-R[f]	+R[g]	AI[h]
rBceCP	505	58.99	4.93	34.55	-0.571	90	63	76.08

can determine the thermostability level of the protein for rBceCP is 76.08 (Table 1), so this protein was likely to be stable over a wide temperature range. In the Kyte-Doolittle Hydropathy Plot, the scale on the x-axis on the left states the hydrophobicity score where a positive number represents amino acid residues that tend to be more hydrophobic and a negative number represents the opposite. The y-axis represents the amino acid sequence that makes up a protein.

In Table 2, it can be seen that the most dominant amino acid constituent of CAP protein from *Bacillus cereus* is glutamic acid with a proportion of 12.3%. Glutamic acid is an amino acid with polar side chains. The polar side chain will be exposed to the outside and interact with water. The large proportion of glutamic acid coupled with other polar amino acid residues (serine, threonine, asparagine, cysteine, aspartic acid, glutamine, arginine, histidine, and lysine) is one of the factors determining the solubility of CAP protein from Bacillus cereus. Among these polar amino acids, aspartic acid, glutamic acid, and serine play the most important role in protein solubility.

3.2. Expression and Purification of rBceCP Protein

The Bceep gene was cloned with a His-tag at the C-terminal and the recombinant plasmid construct was transformed in *E. coli* BL21 (DE3). His-tag is used to purify the Ni-NTA affinity column. IPTG-induced culture results were analyzed using SDS-PAGE and analyzed using ImageJ (Figure 3A). Then, rBceCP protein expression was confirmed using Western blot probed with anti-His antibody (Figure 3B). In *E. coli* BL21(DE3)/pET21b(+)-EntCP, the protein was overexpressed in the lysate fraction with a size of ~60.3 kDa. The expression process was performed by adding IPTG as an inducer with four different concentration variations (0, 0.25, 0.5, and 1 mM) to determine the optimal protein concentration. There were no significant differences between the three IPTG inductions ($p>0.05$). Specifically, the band is only visible in the predicted size of rBceCP and rEntCP as

Table 2. Amino acid composition of CAP protein from *Bacillus cereus*

Amino acid	Proportion (%)
Alanine (A)	5.7
Arginine (R)	4.0
Asparagine (N)	3.8
Aspartic acid (D)	5.5
Cysteine (C)	0.6
Glutamine (Q)	3.6
Glutamic acid (E)	12.3
Glycine (G)	5.7
Histidine (H)	1.8
Isoleucine (I)	4.8
Leucine (L)	9.3
Lysine (K)	8.5
Methionine (M)	3.0
Phenylalanine (F)	5.3
Proline (P)	3.0
Serine (S)	5.0
Threonine (T)	5.3
Tryptophan (W)	1.4
Tyrosine (Y)	6.1
Valine (V)	5.3

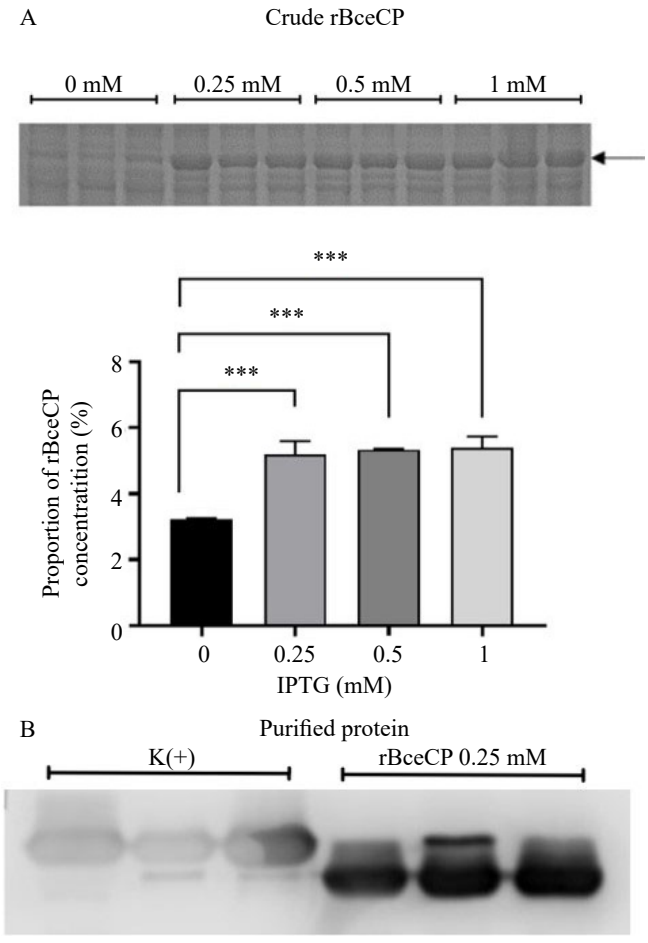

Figure 3. (A) SDS-PAGE result and concentrations of rBceCP in various IPTG concentrations, (B) western blot result of protein samples show overexpressed rBceCP protein at ~60.3 kDa region. The rEntCP was used as the positive control

the positive control. This indicates that a protein with high purity was successfully isolated.

3.3. rBceCP Protein Hydrolysis and Inhibition Activity

When the ACE2-like protein binds and cuts the amino acid lysine located at the carboxyl terminus, the Nma molecule will fluoresce so that it can be detected by a spectrofluorometer, as illustrated in Figure 4. Both samples of crude and purified protein showed similar activity trends.

The inhibitory effect of rBceCP protein on the binding of the SARS-CoV-2 S1 protein to ACE2 was evaluated using the SARS-CoV-2 S1 Protein-ACE2 Binding Inhibitor Screening Kit, employing the ELISA method. The results of the inhibition test conducted with the crude rBceCP protein sample are presented in Figure 5. The crude and purified proteins demonstrated inhibitory activity concerning the binding between SARS-CoV-2 S1 protein and ACE2, with relative inhibition of 47.11% and 50.70%, respectively. The purified protein exhibited a marginally higher inhibitory activity than the protein that did not undergo the purification stage, and a significantly higher inhibitory activity than the positive control (IC) ($p<0.005$). The higher inhibition activity observed in the purified protein may be attributed to the presence of other proteins or molecules that interfere with the binding between the rBceCP protein in the crude sample and the S1 SARS-CoV-2 protein. However, the results of the statistical tests indicate that there is no significant difference between the purified protein samples and those that were not ($p = 0.6114$).

4. Discussion

The molecular characteristics of rBceCP provide insight into its functionality, stability, and potential applications. The α-helix structure pattern of this protein is one of the most common patterns found since they

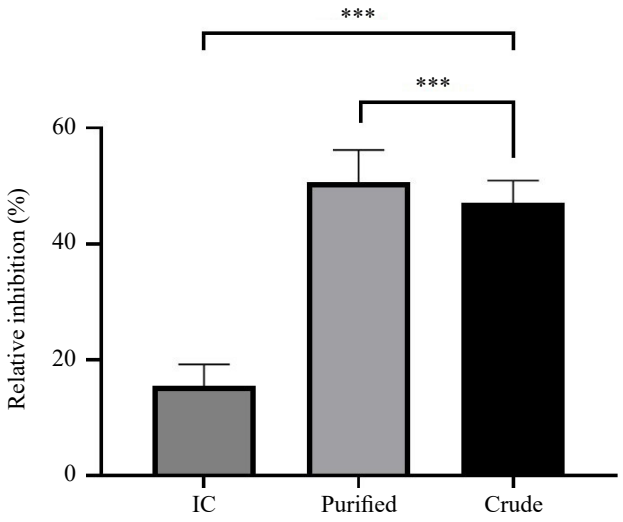

Figure 5. Comparison of inhibitory activity (average) of crude and purified rBceCP protein lysate on the binding of S1 SARS-CoV-2 with ACE2. IC: inhibitor control

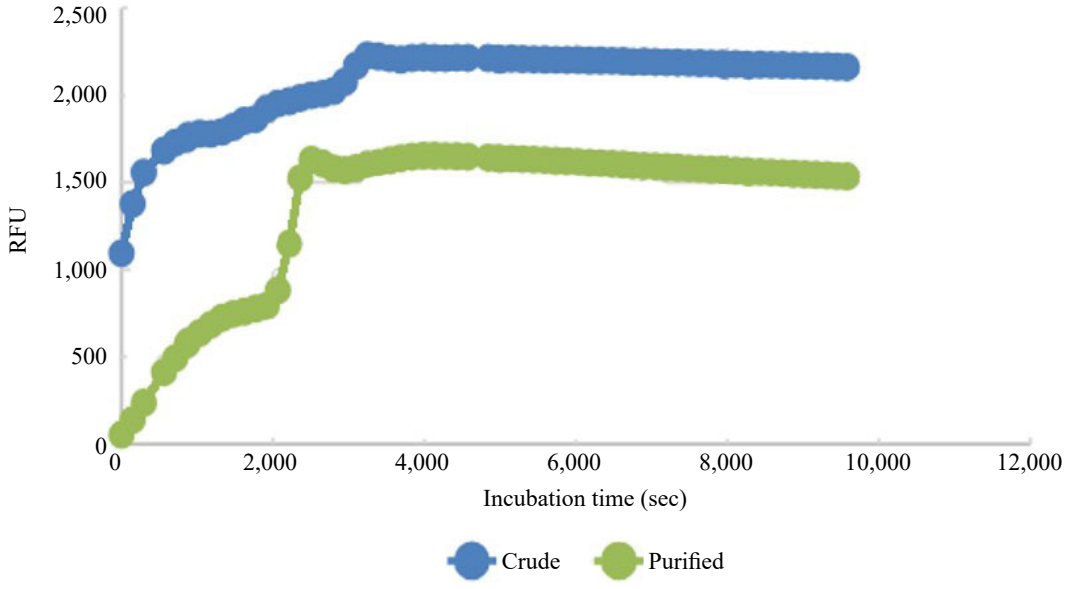

Figure 4. Comparison of protein hydrolysis activity of rBceCP. Crude: cell-free protein extract. Purified: purified protein using Ni-NTA column, as mentioned in the methods section

are formed from hydrogen bonds between C=O groups with N-H groups without involving the side chains of the amino acids that make up the protein. This structure can be formed regardless of the type of amino acids that make up the protein. The α-helix is particularly stable and energetically favorable, contributing significantly to the compact and functional folding of proteins (Alberts *et al.* 2008). The predominance of polar amino acids, particularly glutamic acid (12.3%), serine, and aspartic acid, contributes significantly to the protein's solubility. The polar side chains of these residues are exposed to the aqueous environment, which is essential for protein solubility. If future research seeks to further improve solubility, substituting amino acids like asparagine, glutamine, or threonine with serine, aspartic acid, or glutamic acid (Trevino *et al.* 2007).

The stability of rBceCP is evidenced by a negative GRAVY value, which classifies it as hydrophilic, and an Instability Index (II) of 34.55, categorizing the protein as stable. Stability is a critical factor for its utility in biotechnological processes, such as expression, purification, and crystallization, where maintaining protein structure and function is crucial. The long estimated half-life (>10 hours, Table 3) of rBceCP further supports its potential for in vitro and therapeutic applications, as it suggests prolonged functionality in various cell environments (Panda & Chandra 2012). Additionally, the Aliphatic Index (AI) of 76.08 suggests that the protein is stable over a broad temperature range, enhancing its versatility in different conditions (Deller *et al.* 2016).

The isoelectric point (pI) of rBceCP is 4.93, meaning the protein carries no net charge at this pH, leading to lower solubility (Tokmakov *et al.* 2021). This property is important when considering buffer systems for techniques such as Native PAGE, as maintaining a pH above the pI ensures the protein is charged and can be efficiently separated during electrophoresis. This highlights the importance of careful pH selection in protein purification and characterization protocols.

This study shows the lower hydrolytic activity of purified rBceCP compared to the crude form. At the molecular level, rBceCP contains a conserved active site characteristic of M32-carboxypeptidases, which includes the catalytic residues essential for enzymatic activity. The HEXXH motif (His234 and His238) coordinates the zinc ion at the active site, playing a crucial role in hydrolytic function. Additionally, Arg348, which is analogous to Arg273 in human ACE2, is involved in substrate binding, while other residues such as Tyr424 contribute to the stabilization of the enzyme-substrate complex. The lower activity likely stems from using Ni-NTA affinity chromatography, which may have disrupted the binding of zinc ions, essential cofactors for metalloproteins such as rBceCP. The leaching of these ions from the active site compromises the enzyme's functionality. To resolve this issue, future experiments could incorporate exogenous zinc ions during purification or modify the purification method to prevent metal ion loss. Additionally, expressing the protein as an apoenzyme and reintroducing metal ions through titration may further preserve its activity (Harnden *et al.* 2021). Another solution is to add exogenous zinc ions into the purification buffer to ensure that zinc ions remain bound to the enzyme throughout the purification process. It is also possible to minimize the exposure of the enzyme to conditions that might cause the loss of zinc ions, such as buffers with high concentrations of chloride ions, which can compete with zinc for binding sites on the enzyme, given that this experiment used a chloride-based buffer (Cheng *et al.* 1999).

Table 3. The half-life of rBceCP

Mammalian reticulocytes (*in vitro*)	Yeast (*in vivo*)	*Escherichia coli* (*in vivo*)
30 hours	>20 hours	>20 hours

Interestingly, rBceCP shares structural homology with human ACE2, particularly in the substrate-binding region, suggesting that rBceCP may have ACE2-like properties. The inhibition assay showed that rBceCP could inhibit the interaction between ACE2 and the SARS-CoV-2 spike protein by 52.21%. This opens the possibility of developing rBceCP as a therapeutic agent against COVID-19. The enzyme's ability to interact with the spike protein, potentially blocking viral entry, is a promising avenue for drug development, especially given the ongoing search for effective treatments (Minato *et al.* 2020).

In conclusion, rBceCP demonstrates a combination of favorable properties, including hydrophilicity, stability, and potential therapeutic relevance. The findings suggest that rBceCP could become a valuable tool in biotechnology and a candidate for COVID-19 therapeutic development with further optimization, particularly in purification methods and possibly through protein engineering.

Acknowledgements

We thank Professor Jun Ogawa and Assistant Professor Michiki Takeuchi of Kyoto University, who

provided fluorogenic substrate Nma-His-Pro-Lys(Dnp) and positive control for hydrolysis and inhibitory assay (recombinant EntCP). This research was supported by *Basis Informasi Penelitian dan Pengabdian kepada Masyarakat* (BIMA contract number 110/E5/PG.02.00/PL/2023) The Ministry of Education, Culture, Research, and Technology and *Penelitian, Pengabdian kepada Masyarakat dan Inovasi* ITB (P2MI SK No. 27A/IT1.C11/SK-TA 2023).

References

Alberts, B., Johnson, A., Lewis, J., Raff, M., Roberts, K., Walter, P. 2008. Molecular Biology of the Cell, fourth ed. Garland Science, New York.

Cheng, T.C., Ramakrishnan, V., Chan, S.I. 1999. Purification and characterization of a cobalt-activated carboxypeptidase from the hyperthermophilic archaeon *Pyrococcus furiosus. Protein Science : A Publication of the Protein Society.* 8, 2474. https://doi.org/10.1110/PS.8.11.2474

Deller, M.C., Kong, L., Rupp, B. 2016. Protein stability: a crystallographer's perspective. *Acta Crystallographica. Section F, Structural Biology Communication.* 72, 72–95. https://doi.org/10.1107/S2053230X15024619

Donoghue, M., Hsieh, F., Baronas, E., Godbout, K., Gosselin, M., Stagliano, N., Donovan, M., Woolf, B., Robison, K., Jeyaseelan, R., Breitbart, R.E., Acton, S., 2000. A novel angiotensin-converting enzyme-related carboxypeptidase (ACE2) converts angiotensin I to angiotensin 1-9. *Circulation Research.* 87, 1.9. https://doi.org/10.1161/01.RES.87.5.E1

Fibriani, A., Laily, I.N., Angelina, A., Taharuddin, P., 2022. Isolation and characterization of ACE2-like enzyme from endogenous Indonesian microorganism in fermented food as an alternative treatment for COVID-19. *J-Stage*. 91, 106. https://doi.org/10.50867/AFREPORT.2022_106

Harnden, K. A., Roy, A., Hosseinzadeh, P., 2021. Overview of methods for purification and characterization of metalloproteins. *Current Protocols*. 1, 1-14. https://doi.org/10.1002/CPZ1.234

Imai, Y., Kuba, K., Rao, S., Huan, Y., Guo, F., Guan, B., Yang, P., Sarao, R., Wada, T., Leong-Poi, H., Crackower, M. A., Fukamizu, A., Hui, C.C., Hein, L., Uhlig, S., Slutsky, A.S., Jiang, C., Penninger, J.M., 2005. Angiotensin-converting enzyme 2 protects from severe acute lung failure. *Nature*. 436, 112–116. https://doi.org/10.1038/nature03712

Khan, A., Benthin, C., Zeno, B., Albertson, T.E., Boyd, J., Christie, J.D., Hall, R., Poirier, G., Ronco, J.J., Tidswell, M., Hardes, K., Powley, W.M., Wright, T.J., Siederer, S.K., Fairman, D.A., Lipson, D.A., Bayliffe, A.I., Lazaar, A.L. 2017. A pilot clinical trial of recombinant human angiotensin-converting enzyme 2 in acute respiratory distress syndrome. *Critical Care*. 21, 234. https://doi.org/10.1186/S13054-017-1823-X

Laily, I.N., Takeuchi, M., Mizutani, T., Ogawa, J., 2023. An ACE2, SARS-CoV-2 spike protein binding protein, -like enzyme isolated from food-related microorganisms. *Bioscience, Biotechnology, and Biochemistry*. 87, 638–645. https://doi.org/10.1093/BBB/ZBAD037

Meyer, N.J., Gattinoni, L., Calfee, C.S. 2021. Acute respiratory distress syndrome. *Lancet*. 398, 622–637. https://doi.org/10.1016/S0140-6736(21)00439-6

Minato, T., Nirasawa, S., Sato, T., Yamaguchi, T., Hoshizaki, M., Inagaki, T., Nakahara, K., Yoshihashi, T., Ozawa, R., Yokota, S., Natsui, M., Koyota, S., Yoshiya, T., Yoshizawa-Kumagaye, K., Motoyama, S., Gotoh, T., Nakaoka, Y., Penninger, J. M., Watanabe, H., Imai, Y,. Takahashi, S., Kuba, K., 2020. B38-CAP is a bacteria-derived ACE2-like enzyme that suppresses hypertension and cardiac dysfunction. *Nature Communications.* 11, 1058. https://doi.org/10.1038/S41467-020-14867-Z

Minato, T., Yamaguchi, T., Hoshizaki, M., Nirasawa, S., An, J., Takahashi, S., Penninger, J. M., Imai, Y., Kuba, K., 2022. ACE2-like enzyme B38-CAP suppresses abdominal sepsis and severe acute lung injury. *PLoS ONE.* 17, 1-13. https://doi.org/10.1371/JOURNAL.PONE.0270920

Muslim, S., Nasrin, N., Alotaibi, F. O., Prasad, G., Singh, S. K., Alam, I., Mustafa, G., 2020. Treatment options available for COVID-19 and an analysis on possible role of combination of rhACE2, angiotensin (1-7) and angiotensin (1-9) as effective therapeutic measure. *SN Comprehensive Clinical Medicine.* 2, 1761–1766. https://doi.org/10.1007/S42399-020-00407-9

Panda, S., Chandra, G., 2012. Physicochemical characterization and functional analysis of some snake venom toxin proteins and related non-toxin proteins of other chordates. *Bioinformation*. 8, 891–896. https://doi.org/10.6026/97320630008891

Satyanarayana, S.D.V., Krishna, M.S.R., Pavan Kumar, P., Jeereddy, S., 2018. *In silico* structural homology modeling of nif A protein of rhizobial strains in selective legume plants. *Journal of Genetic Engineering and Biotechnology*. 16, 731–737. https://doi.org/10.1016/J.JGEB.2018.06.006

Tipnis, S.R., Hooper, N.M., Hyde, R., Karran, E., Christie, G., Turner, A.J., 2000. A human homolog of angiotensin-converting enzyme. Cloning and functional expression as a captopril-insensitive carboxypeptidase. *The Journal of Biological Chemistry*. 275, 33238–33243. https://doi.org/10.1074/JBC.M002615200

Tokmakov, A.A., Kurotani, A., Sato, K.I., 2021. Protein pI and intracellular localization. *Frontiers in Molecular Biosciences*. 8, 775736. https://doi.org/10.3389/FMOLB.2021.775736/BIBTEX

Trevino, S.R., Scholtz, J.M., Pace, C.N., 2007. Amino acid contribution to protein solubility: Asp, Glu, and Ser contribute more favorably than the other hydrophilic amino acids in RNase Sa. *Journal of Molecular Biology.* 366, 449–460. https://doi.org/10.1016/J.JMB.2006.10.026

Yamaguchi, T., Hoshizaki, M., Minato, T., Nirasawa, S., Asaka, M.N., Niiyama, M., Imai, M., Uda, A., Chan, J.F.W., Takahashi, S., An, J., Saku, A., Nukiwa, R., Utsumi, D., Kiso, M., Yasuhara, A., Poon, V.K.M., Chan, C.C.S., Fujino, Y., Motoyama, S., Nagata, S., Penninger, J.M., Kamada, H., Yuen, K.Y., Kamitani, W., Maeda, K., Kawaoka, Y., Yasutomi, Y., Imai, Y., Kuba, K., 2021. ACE2-like carboxypeptidase B38-CAP protects from SARS-CoV-2-induced lung injury. *Nature Communications*. 12, 1–13. https://doi.org/10.1038/s41467-021-27097-8

Yang, X., Yu, Y., Xu, J., Shu, H., Xia, J., Liu, H., Wu, Y., Zhang, L., Yu, Z., Fang, M., Yu, T., Wang, Y., Pan, S., Zou, X., Yuan, S., Shang, Y., 2020. Clinical course and outcomes of critically ill patients with SARS-CoV-2 pneumonia in Wuhan, China: a single-centered, retrospective, observational study. *The Lancet. Respiratory Medicine.* 8, 475–481. https://doi.org/10.1016/S2213-2600(20)30079-5